Plasma Sources Sci. Technol. **20** (2011) 045007 (13pp) doi:10.1088/0963-0252/20/4/045007

Secondary electrons in dual-frequency capacitive radio frequency discharges

J Schulze[1,2], Z Donkó[1], E Schüngel[2] and U Czarnetzki[2]

[1] Research Institute for Solid State Physics and Optics, Hungarian Academy of Sciences, Budapest, Hungary
[2] Institute for Plasma and Atomic Physics, Ruhr-University Bochum, Germany

E-mail: fjschulze@hotmail.com

Received 20 December 2010, in final form 18 April 2011
Published 31 May 2011
Online at stacks.iop.org/PSST/20/045007

Abstract
Two fundamentally different types of dual-frequency (DF) capacitively coupled radio frequency discharges can be used for plasma processing applications to realize separate control of the ion mean energy, $\langle E_i \rangle$, and the ion flux, Γ_i, at the substrate surface: (i) classical discharges operated at substantially different frequencies, where the low- and high-frequency voltage amplitudes, ϕ_{lf} and ϕ_{hf}, are used to control $\langle E_i \rangle$ and Γ_i, respectively; (ii) electrically asymmetric (EA) discharges operated at a fundamental frequency and its second harmonic with fixed, but adjustable phase shift between the driving frequencies, θ. In EA discharges the voltage amplitudes are used to control Γ_i and θ is used to control $\langle E_i \rangle$. Here, we report our systematic simulation studies of the effect of secondary electrons on the ionization dynamics and the quality of this separate control in both discharge types in argon at different gas pressures. We focus on the effect of the control parameter for $\langle E_i \rangle$ on Γ_i for different secondary yields, γ. We find a dramatic effect of tuning ϕ_{lf} in classical DF discharges, which is caused by a transition from α- to γ-mode induced by changing ϕ_{lf}. In EA discharges we find that no such mode transition is induced by changing θ within the parameter range studied here and, consequently, Γ_i remains nearly constant as a function of θ. Thus, despite some limitations at high values of γ the quality of the separate control of ion energy and flux is generally better in EA discharges compared with classical DF discharges.

(Some figures in this article are in colour only in the electronic version)

1. Introduction

Separate control of the mean ion energy, $\langle E_i \rangle$, and the ion flux, Γ_i, at the electrode surfaces in capacitively coupled radio frequency (CCRF) discharges is an important issue for various applications of plasma processing [1, 2]. For instance, in the frame of plasma-enhanced chemical vapor deposition processes such as used for solar cell manufacturing, this separate control is most relevant. It principally allows one to increase Γ_i to realize high process rates, while $\langle E_i \rangle$ is kept constant at low values to prevent highly energetic ion bombardment of the substrate to avoid unwanted damage of the surface structure [3–5].

In single frequency CCRF discharges this separate control cannot be realized, since a change in the amplitude of the applied voltage waveform affects both $\langle E_i \rangle$ and Γ_i. Instead, either hybrid discharges (RF-DC [6–8], capacitive-helicon [9, 10], capacitive-inductive [10–12]) or dual-frequency (DF) CCRF discharges are used to decouple $\langle E_i \rangle$ and Γ_i. There are two fundamentally different types of DF discharges: (i) classical discharges operated at substantially different frequencies [13–24], e.g. 2 and 27 MHz, and (ii) electrically asymmetric (EA) discharges operated at a fundamental frequency and its second harmonic, e.g. 13.56 and 27.12 MHz, with fixed, but adjustable phase shift, θ, between the driving frequencies [25–38]. Classical DF discharges are frequently used for industrial applications, whereas the alternative concept of EA discharges has recently been proposed based on the discovery of the electrical asymmetry effect (EAE) and only prototypes have been built until now [29, 36].

In classical DF discharges one electrode is driven by the following voltage waveform, $\tilde{\phi}(t)$, with $\omega_{hf} \gg \omega_{lf}$:

$$\tilde{\phi}(t) = \phi_{lf} \cos(\omega_{lf} t) + \phi_{hf} \cos(\omega_{hf} t). \quad (1)$$

Here, t is time, ϕ_{lf}, ϕ_{hf} is the low- and high-frequency voltage amplitude, respectively, $\omega_{lf} = 2\pi f_{lf}$ and $\omega_{hf} = 2\pi f_{hf}$, where f_{lf}, f_{hf} is the low and high driving frequency, respectively. Typical driving frequencies are $f_{lf} = 1$–2 MHz and $f_{hf} = 27$–100 MHz. In these discharges, the fundamental idea to control $\langle E_i \rangle$ separately from Γ_i is based on choosing $\phi_{lf} \gg \phi_{hf}$ to ensure that the ion acceleration inside the sheaths, and thus $\langle E_i \rangle$, are controlled only by the low-frequency (lf) voltage amplitude. Due to the large difference of the driving frequencies and the more effective electron heating at higher frequencies, the high-frequency (hf) voltage amplitude should control the ion flux at the electrodes. However, the coupling of both frequencies was demonstrated to limit the quality of the separate control in these discharges [39–46]. Moreover, recent simulations and experiments indicated even stronger limitations due to the effect of secondary electrons [44, 47].

In EA DF discharges one electrode is driven by the superposition of a fundamental frequency and its second harmonic, i.e. the following driving voltage waveform is used:

$$\tilde{\phi}(t) = \phi_{lf} \cos(\omega_{lf} t + \theta) + \phi_{hf} \cos(2\omega_{lf} t). \quad (2)$$

Here, θ is the fixed, but adjustable, phase shift between the driving harmonics. Typically, $f_{lf} = 13.56$ MHz is used. The concept to control the mean ion energies at the electrodes separately from the ion flux in these discharges is fundamentally different from the concept used in classical DF discharges. Here, the voltage amplitudes are kept constant and only the relative phase between the driving frequencies, θ, is changed to control the ion energy. In this way any frequency coupling is avoided. Tuning θ results in the electrical generation of a variable dc self-bias, η, that depends almost linearly on θ due to the EAE even in geometrically symmetric discharges. Thus, the mean ion energies at the electrodes can be controlled by tuning θ such as demonstrated experimentally and by particle-in-cell simulations complemented with Monte Carlo treatment of collision processes (PIC/MCC) without discussing the effect of secondary electrons [27, 29]. The ion flux is controlled by adjusting the voltage amplitudes.

Secondary electrons generated by ion bombardment at the electrodes with a yield γ play an important role in single [48] and classical DF CCRF discharges [41, 44, 49]. Typically, $\gamma = 0 - 0.5$ depending on the electrode/wafer material and the surface conditions [50, 51]. These γ-electrons are known to induce transitions of the electron heating mode from α- to γ-mode at high driving voltage amplitudes and/or pressures [48]. In α-mode, the plasma density and the ion fluxes to the electrodes are low and the ionization dynamics is typically dominated by energetic electron beams generated by the expanding sheaths [52–57]. In γ-mode the plasma density and the ion fluxes to the electrodes are substantially higher and the ionization dynamics is dominated by secondary electrons [48].

Different effects of the control parameter for $\langle E_i \rangle$ on Γ_i were observed in classical DF discharges: using PIC/MCC simulations and neglecting secondary electrons ($\gamma = 0$) Donkó *et al* [45, 46] found the ion flux to decrease as a function of ϕ_{lf} in an argon discharge operated at 1 + 100 MHz, while Boyle *et al* [58] found it to remain constant at about 6.6 Pa. At high values of γ, Booth *et al* [47] experimentally observed Γ_i to increase as a function of ϕ_{lf} in a mixture of argon and oxygen at the same pressure. Georgieva and Bogaerts [59] found a complicated dependence of Γ_i on ϕ_{lf} in Ar/CF_4/N_2 using simulations. Recently, Donkó *et al* [44] investigated the effect of secondary electrons on the quality of the separate control of $\langle E_i \rangle$ and Γ_i in classical DF discharges operated at 1.937 + 27.12 MHz and resolved this mystery of apparently oppositional results. They found Γ_i to decrease as a function of ϕ_{lf} at low values of γ, to remain constant at intermediate values and to increase as a function of ϕ_{lf} at high values of γ.

Based on these results, in this paper we perform a detailed analysis of the effect of secondary electrons on the ionization dynamics and the separate control of ion properties in (i) classical as well as (ii) EA DF discharges and (iii) we compare our results for both discharge types to conclude which type allows a better separate control. For both discharge types, we investigate different gas pressures of 6.6, 20 and 100 Pa by simulations. We focus on the effect of changing the control parameter for the mean ion energy on the ionization dynamics and the ion flux at the electrodes for different values of γ and compare our results with those obtained in previous experimental and simulation works. Ideally, changing the control parameter for $\langle E_i \rangle$ should not affect Γ_i. We will explore to what extent and why this principle is fulfilled or violated by the effect of secondary electrons in both discharge types.

The paper is structured in the following way: in the second section, details of the simulation method are introduced. In the third section, the results are presented. This section is divided into three parts: first, the ionization dynamics and the quality of the separate control of ion energy and flux at the electrodes in classical DF discharges are analyzed for different values of γ and ϕ_{lf}, while ϕ_{hf} is kept constant at each pressure. In the second part, EA DF discharges are investigated with respect to the ionization dynamics and the quality of the separate control under variation of γ and θ at fixed voltage amplitudes at each neutral gas pressure. In the third part, the results for both discharge types are compared with respect to the quality of the separate control of ion properties. Conclusions are drawn in section 4.

2. Simulation method

We use an electrostatic particle-in-cell simulation complemented with Monte Carlo treatment of collision processes (PIC/MCC). The code is one dimensional in space and three dimensional in velocity space; the electrodes are infinite, plane, and separated by a distance $d = 2.5$ cm. All discharges investigated are geometrically symmetric, i.e. the electrode surface areas are identical. The simulations are performed in argon with a gas temperature of 400 K at different values of γ. The number of superparticles is kept constant at approximately 1×10^5 per particle species for all conditions investigated with about 500 superparticles per species and Debye length. Electrons are reflected at the electrodes with a probability of 20% [60]. The cross sections for electron–neutral and ion–neutral collisions are taken from [51, 61, 62].

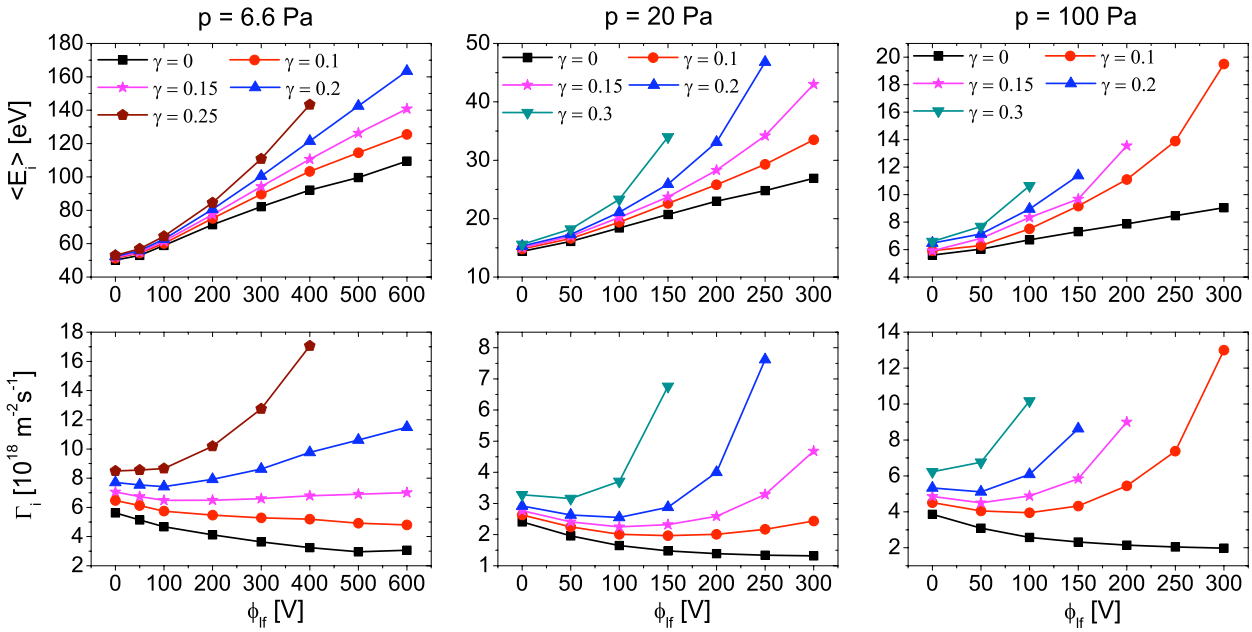

Figure 1. Mean ion energy ($\langle E_\mathrm{i}\rangle$: first row) and ion flux (Γ_i: second row) at the electrodes as a function of ϕ_lf at different pressures (6.6, 20, 100 Pa) and different values of γ in classical DF discharges. Discharge conditions: $f_\mathrm{hf} = 27.12$ MHz, $f_\mathrm{lf} = f_\mathrm{hf}/14 \approx 1.937$ MHz, argon, 2.5 cm electrode gap. ϕ_hf is kept constant at 200 V, 100 V and 100 V at 6.6 Pa, 20 Pa and 100 Pa, respectively. Partly reproduced from [44].

As secondary electrons may be accelerated inside the sheaths to a maximum velocity $v_\mathrm{max} = \sqrt{2q(\phi_\mathrm{hf} + \phi_\mathrm{lf})/m}$, a very small time step ($\Delta t \leqslant \Delta x/v_\mathrm{max}$) is required to fulfil the Courant condition. Here Δx is the division of the computational grid, m and q are the electron mass and the elementary charge. Time-synchronized PIC schemes are inefficient at this point, since the number of γ-electrons is typically small compared with the number of 'slow' electrons; the tracing of the latter would allow much longer time steps. Therefore, in our code we treat fast and slow electrons as different species and use different time steps to fulfil the Courant condition. The electrons emitted from the electrodes and those originating from ionization processes are initially treated as fast electrons and will be transferred to the group of slow electrons, if their energy falls below a threshold (15 eV) in the central region of the discharge.

For our investigations of classical DF discharges we apply a voltage waveform according to equation (1) to one electrode. We keep ϕ_hf constant and change γ from 0 to 0.3 and ϕ_lf from 0 V to $3\phi_\mathrm{hf}$. In the case of EA DF discharges we use a driving voltage waveform according to equation (2) with $\phi_\mathrm{lf} = \phi_\mathrm{hf}$ and change γ from 0 to 0.4 and θ from 0° to 90°. For each discharge type we perform simulations at 6.6, 20 and 100 Pa in argon. In this way, we study almost collisionless discharge conditions (6.6 Pa), where the electron ionization mean free path, λ_e, is comparable to the bulk length, l, collisional conditions (100 Pa), where λ_e is smaller than the maximum sheath width, s_max, and an intermediate regime (20 Pa).

3. Results

3.1. Classical DF discharge

Figure 1 shows the mean energy, $\langle E_\mathrm{i}\rangle$, and the flux, Γ_i, of argon ions at the electrodes as a function of the lf voltage amplitude, ϕ_lf, at different pressures (6.6, 20 and 100 Pa) and secondary yields, γ, in a discharge operated at $f_\mathrm{hf} = 27.12$ MHz and $f_\mathrm{lf} = f_\mathrm{hf}/14 \approx 1.937$ MHz. The hf voltage amplitude, ϕ_hf, is kept constant at 200 V, 100 V and 100 V at 6.6 Pa, 20 Pa and 100 Pa, respectively. Different values of ϕ_hf are used at different pressures in order to ensure convergence of the simulation for a large number of combinations of γ and ϕ_lf at a given pressure. This requires higher voltages at lower pressures. Due to the discharge symmetry, there is no dc self-bias, η, and the mean ion energies as well as the ion fluxes are identical at both electrodes, respectively.

Essentially the same trends are observed at all three neutral gas pressures: for all values of γ, the mean ion energy increases as a function of ϕ_lf, i.e. the lf voltage amplitude is an efficient control parameter for $\langle E_\mathrm{i}\rangle$. The mean ion energy also increases as a function of γ at fixed ϕ_lf. This is caused by a decrease in the sheath width as a function of γ due to the increased plasma density. Thus, at a given pressure and mean free path, the ions undergo fewer collisions inside the sheaths and arrive at the electrodes at higher energies. This effect might be the basis of a novel *in situ* technique to determine γ-coefficients from the comparison of $\langle E_\mathrm{i}\rangle$ obtained from experiment and simulation.

Under most discharge conditions the ion flux (second row in figure 1) is not constant as a function of ϕ_lf, i.e. the control parameter for $\langle E_\mathrm{i}\rangle$ also affects Γ_i and separate control of ion energy and flux at the electrodes is not possible in most cases: for $\gamma = 0$, the ion flux will decrease as a function of ϕ_lf by a factor of about 2 at all pressures investigated, if ϕ_lf is increased from 0 V to $3\phi_\mathrm{hf}$. This is similar to previous results [45, 46] and is caused by the frequency coupling in classical DF discharges [39–43] and by a constriction of the plasma bulk as a function of ϕ_lf. This coupling effect is illustrated in figures 2(*a*) and (*b*) for an argon discharge operated at 20 Pa as an example. These figures show the spatio-temporal distributions of the ionization

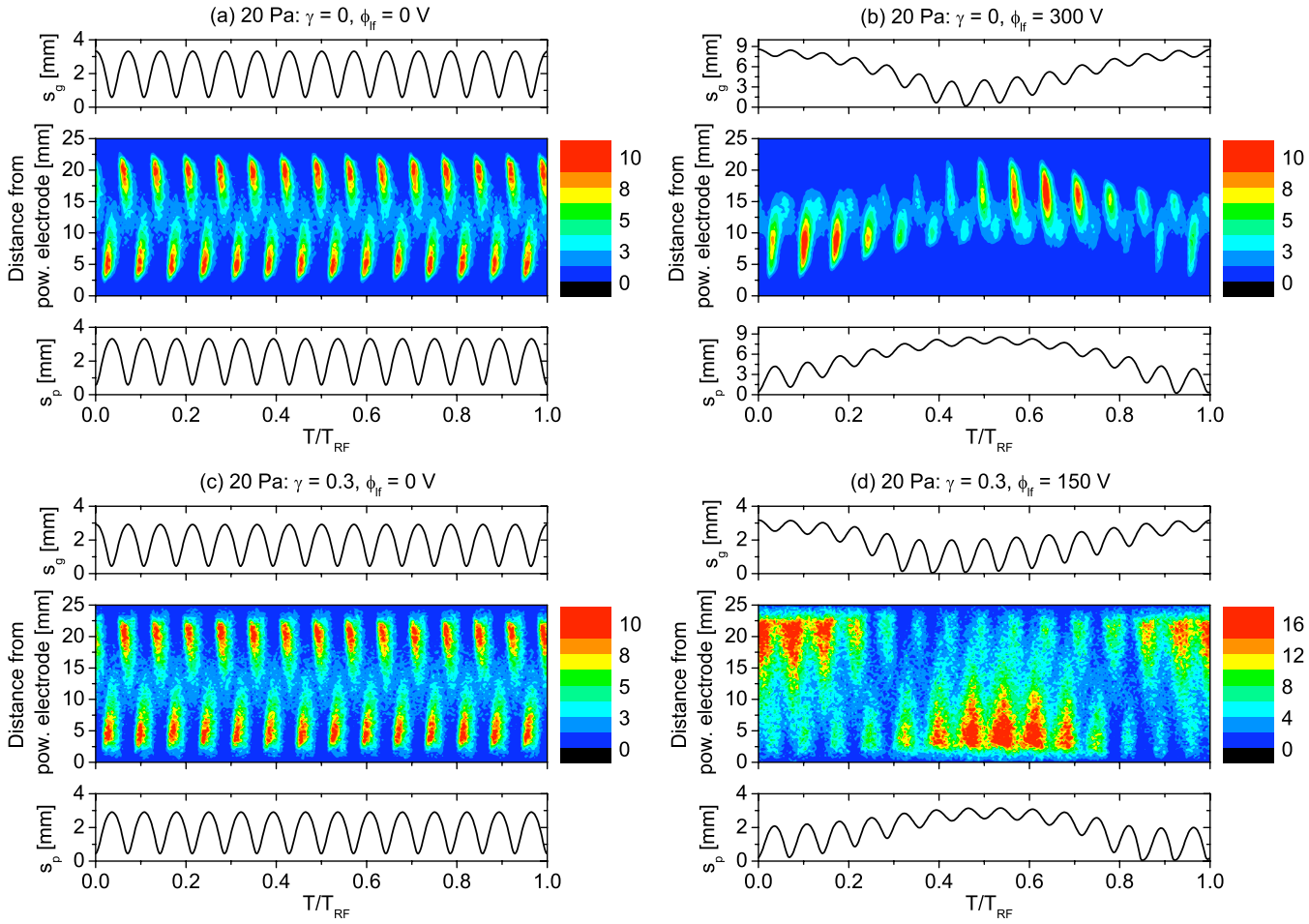

Figure 2. Spatio-temporal distribution of the ionization rate and sheath widths (s_p, s_g) at the powered and grounded electrode as a function of time within one lf period in a classical DF discharge operated in argon at 20 Pa for different values of γ and ϕ_{lf} (2.5 cm electrode gap, $\phi_{hf} = 100$ V): (*a*) $\gamma = 0$, $\phi_{lf} = 0$ V, (*b*) $\gamma = 0$, $\phi_{lf} = 300$ V, (*c*) $\gamma = 0.3$, $\phi_{lf} = 0$ V, (*d*) $\gamma = 0.3$, $\phi_{lf} = 150$ V. The color scale is given in 10^{20} m^{-3} s^{-1}.

rate and sheath widths at both electrodes within one lf period. The sheath widths are calculated according to Brinkmann [63]:

$$\int_0^s n_e(x)\,dx = \int_s^{d/2} (n_i(x) - n_e(x))\,dx. \qquad (3)$$

Here n_e and n_i are the electron and ion densities, respectively, x is the distance from the respective electrode and d is the electrode gap.

For $\gamma = 0$ the discharge is operated in α-mode, i.e. energetic electron beams generated by the expanding sheaths dominate the ionization. Based on the theory of stochastic heating in CCRF discharges [1, 64] the drift velocity of these beam electrons is determined by the sheath expansion velocity. By increasing ϕ_{lf} the oscillating sheath edge is pushed away from the electrode into a region of higher ion density during most of one lf period. This reduces the sheath expansion velocity and, thus, the ionization at times, when the sheath oscillates in high-density regions. Consequently, for $\gamma = 0$ the ion flux decreases as a function of ϕ_{lf}.

Similar to the experimental results of Booth *et al* [47] the ion flux strongly increases as a function of ϕ_{lf} for high values of γ, since the ionization by secondary electrons is strongly enhanced as a function of ϕ_{lf}. This is illustrated in figures 2(*c*) and (*d*) at $\gamma = 0.3$: for $\phi_{lf} = 0$ V a pattern of the spatio-temporal ionization rate similar to figure 2(*a*) is observed, i.e. the ionization maxima occur at the same times and are similarly strong. A weak broadening of the maxima due to additional ionization by secondary electrons accelerated in the hf sheath is observed. Nevertheless, the discharge is essentially operated in α-mode. Increasing ϕ_{lf} causes the secondary electrons to gain more energy and to be multiplied inside the sheaths more efficiently, since the sheath voltages and widths (for a given ion density profile) increase as a function of ϕ_{lf} [48]. For $\phi_{lf} = 150$ V (figure 2(*d*)) the ionization caused by the expanding sheaths, that dominates in α-mode, is hardly visible. Instead, ionization by secondary electrons at the sheath edges adjacent to both electrodes at the times of high sheath voltage dominates. The hf modulation of these ionization maxima is caused by the hf modulation of the sheath potential and is significantly less pronounced compared with the hf modulation of the ionization rate in α-mode. Consequently, a mode transition from α- to γ-mode is induced by changing ϕ_{lf}. Due to this mode transition the ionization and, thus, the ion flux strongly increase as a function of ϕ_{lf} and separate control of ion energy and flux is no longer possible, since the control parameter for $\langle E_i \rangle$ significantly affects Γ_i. This

dramatic effect of secondary electrons is particularly strong for $\phi_{lf} > \phi_{hf}$, i.e. the typical choice of voltage amplitudes in classical DF discharges to realize separate control of ion energy and flux. At high pressures this mode transition occurs at lower ϕ_{lf} at fixed γ and lower γ at fixed ϕ_{lf} due to the shorter electron mean free path and the more effective multiplication of secondary electrons inside the sheaths. For the same reason, the number of superparticles diverges in the simulation at the highest values of γ and pressure, which in an experiment would correspond to instabilities and arc formation. Due to the higher value of ϕ_{hf} at 6.6 Pa, the effective acceleration of secondary electrons inside the sheaths leads to a divergence of the number of superparticles at $\gamma = 0.3$ already for low values of ϕ_{lf}. Thus, the highest secondary electron emission coefficient investigated at 6.6 Pa is $\gamma = 0.25$.

In conclusion, for low values of γ the ion flux decreases as a function of ϕ_{lf} due to the frequency coupling and the constriction of the plasma bulk, and separate control of $\langle E_i \rangle$ and Γ_i is limited. For high values of γ an increase in ϕ_{lf} induces a mode transition from α- to γ-mode causing a strong increase in Γ_i, which is the strongest for voltage amplitudes typically used in classical DF discharges ($\phi_{lf} > \phi_{hf}$). This effect will make a separate control of ion energy and flux impossible in classical DF discharges, if secondary electrons play an important role. In between, there is a rather narrow process window, where the effects of the frequency coupling and the secondary electrons compensate and separate control is possible.

3.2. *Electrically asymmetric dual-frequency discharge*

Figure 3 shows our simulation results for EA DF discharges, i.e. the mean ion energy at the grounded and powered electrode ($\langle E_{i,g} \rangle$: first row, $\langle E_{i,p} \rangle$: second row), the ion fluxes at both electrodes ($\Gamma_{i,g}$: third row, $\Gamma_{i,p}$: fourth row), as well as the dc self-bias normalized by $\phi_{lf} + \phi_{hf}$ ($\bar{\eta}$: fifth row) as a function of the phase shift between the driving harmonics, θ, at different pressures (6.6, 20 and 100 Pa) and secondary yields γ. The discharge is geometrically symmetric and operated at 13.56 and 27.12 MHz. The harmonics' voltage amplitudes are kept constant at $\phi_{lf} = \phi_{hf} = 300$ V, 150 V and 75 V at 6.6 Pa, 20 Pa and 100 Pa, respectively. Similar to the simulations of classical df discharges lower voltages (with identical harmonics amplitudes) had to be used at higher pressures in order to ensure convergence of the simulations for the values of γ studied. Here, θ instead of ϕ_{lf} is used as the control parameter for the mean ion energy at both electrodes. Due to the electrical discharge asymmetry the mean ion energies and the ion fluxes are no longer identical at both electrodes. In contrast to classical DF discharges a dc self-bias is generated as an almost linear function of θ via the EAE [25–38] for all the different values of pressure and γ (last row of figure 3).

Under all conditions investigated the mean ion energies at the electrodes can be changed by tuning θ from 0° to 90°. Tuning θ affects $\langle E_{i,g} \rangle$ and $\langle E_{i,p} \rangle$ in an opposite way, i.e. the role of both electrodes can be reversed [27, 29]. Due to the self-amplification of the EAE [26] a stronger dc self-bias is generated at lower pressures, i.e. the control range for the mean ion energy changes from a factor of about 1.5 at 100 Pa to a factor of about 2.4 at 6.6 Pa. Similar to classical DF discharges we find the mean ion energies at both electrodes to increase as a function of γ at fixed θ. For a given θ, the ion fluxes at both electrodes increase as a function of γ due to the additional ionization by secondary electrons. Depending on the neutral gas pressure different effects of the control parameter for the mean ion energy, θ, on the ion fluxes at the electrodes are found. We start with an analysis of the results at the intermediate pressure of 20 Pa ($s_{max} < \lambda_e < l$): at this pressure, $\Gamma_{i,g}$ and $\Gamma_{i,p}$ will change by a maximum of about 27%, if $\langle E_{i,g} \rangle$ and $\langle E_{i,p} \rangle$ are switched from their minimum to their maximum by changing θ from 0° to 90°, i.e. the ion flux is essentially constant. Except for a small shift due to a change in the dc self-bias and the sheath widths as a function of θ, the ion density profile (figure 4) will remain almost unchanged, if θ is tuned.

In comparison with classical DF discharges the quality of the separate control of ion properties is significantly improved in EA DF discharges due to the fundamentally different concept to control the mean ion energy by tuning θ at fixed voltage amplitudes instead of changing one voltage amplitude at a fixed phase shift between the driving frequencies. While a change in ϕ_{lf} in classical DF discharges induces a mode transition of the ionization dynamics (figure 2), adjusting θ in EA DF discharges does not change the heating mode. Figure 5 shows the spatio-temporal distribution of the ionization rate and the sheath widths at the powered and grounded electrodes as a function of time within one lf period at 20 Pa for $\gamma = 0$ ($\theta = 0°, 90°$) and $\gamma = 0.3$ ($\theta = 0°, 90°$). For $\gamma = 0$, the discharge is operated in α-mode independently of the choice of θ, while it is operated in γ-mode for $\gamma = 0.3$ for all θ. In contrast to classical DF discharges, changing θ affects only the symmetry of the spatio-temporal distribution of the ionization rate [33], but does not change the heating mode for a given γ. Therefore, the control parameter for the mean ion energy affects the ion flux much less than in classical DF discharges discussed in section 3.1.

Next, we discuss the effect of tuning θ on the ion flux at the highest pressure investigated (100 Pa: $\lambda_e < s_{max} < l$); in contrast to the situation at 20 Pa, we find the ion flux at both electrodes to change by about 50%, if θ is tuned from 0° to 90° (figure 3). This quality of the separate control of the mean ion energy and flux is comparable to classical DF discharges (figure 1) for most values of γ. This reduced quality is understood by an analysis of the ionization dynamics shown in figure 6. Again, tuning θ does not change the heating mode. For $\gamma = 0$ the discharge is operated in α-mode for all θ, while it is operated in γ-mode independently of θ for $\gamma = 0.3$. However, the symmetry of the ionization dynamics is changed as a function of θ [33]: for all values of γ most of the ionization happens close to the bottom electrode at $\theta = 0°$, while it occurs close to the top electrode at $\theta = 90°$ (asymmetric ionization). At $\theta \approx 60°$ the ionization is equally strong adjacent to both electrodes (symmetric ionization). Due to the short electron mean free path, the ionization sources are significantly more localized at the sheath edges compared with lower pressures (figures 5 and 7). Thus, in this local regime the symmetry change of the ionization dynamics induced by changing θ

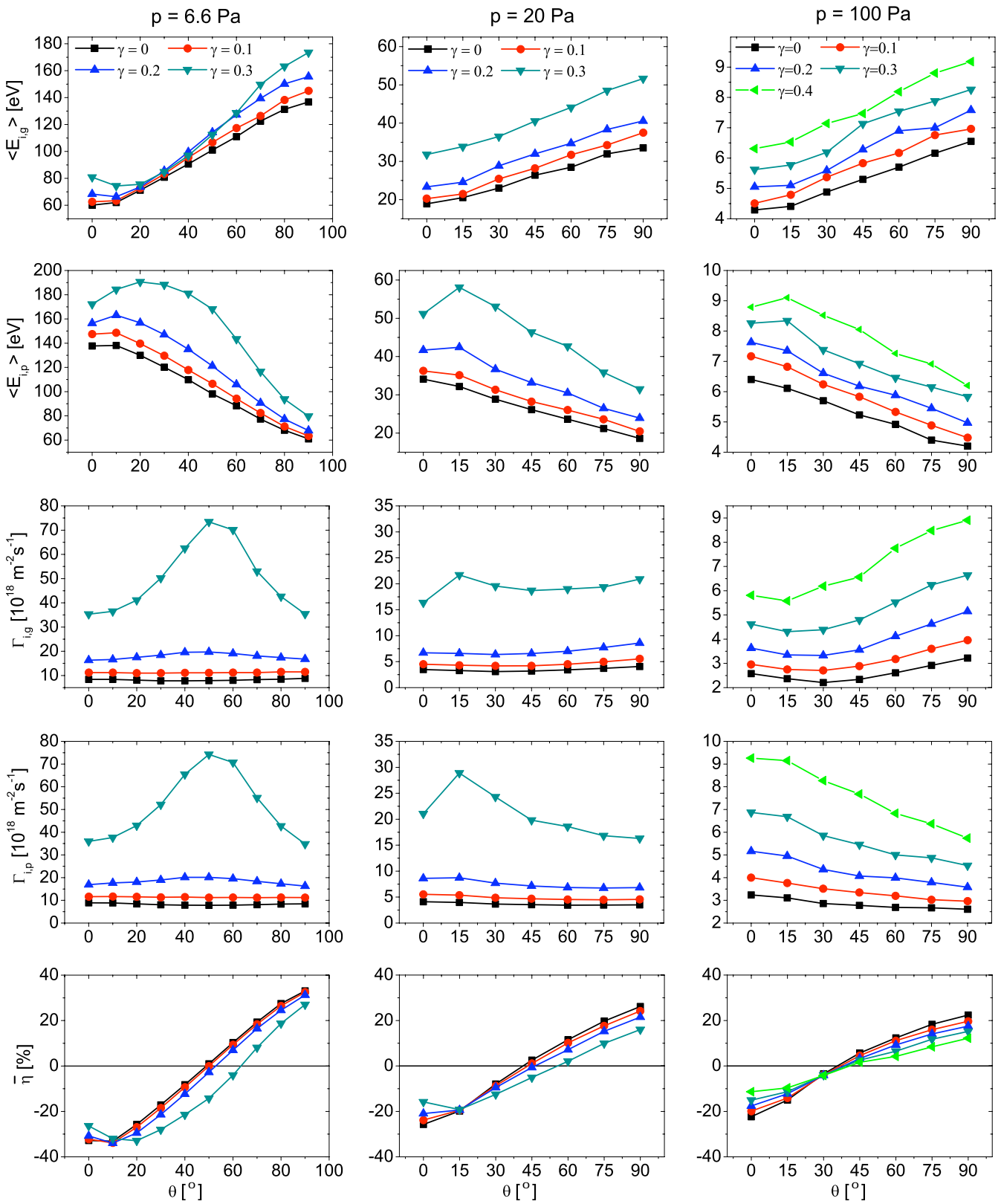

Figure 3. Mean ion energy at the grounded ($\langle E_{\mathrm{i,g}}\rangle$: first row), and powered electrode ($\langle E_{\mathrm{i,p}}\rangle$: second row), as well as the ion flux at the grounded ($\Gamma_{\mathrm{i,g}}$: third row) and powered electrode ($\Gamma_{\mathrm{i,p}}$: fourth row), and the dc self-bias normalized by $\phi_{\mathrm{lf}} + \phi_{\mathrm{hf}}$ ($\bar{\eta}$: fifth row) as a function of θ at different pressures (6.6, 20 and 100 Pa) and different values of γ in electrically asymmetric DF discharges. Discharge conditions: 13.56 + 27.12 MHz, argon, 2.5 cm electrode gap, $\phi_{\mathrm{lf}} = \phi_{\mathrm{hf}}$ are kept constant at 300 V, 150 V and 75 V at pressures of 6.6 Pa, 20 Pa and 100 Pa, respectively.

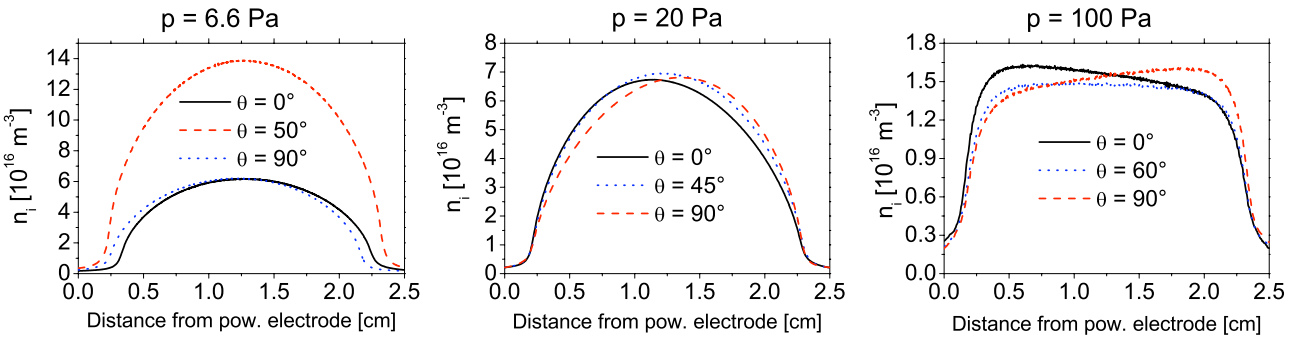

Figure 4. Time-averaged ion density as a function of the distance from the powered electrode for different phase shifts, θ, and for the highest values of γ investigated at 6.6 Pa ($\gamma = 0.3$), 20 Pa ($\gamma = 0.3$) and 100 Pa ($\gamma = 0.4$). Discharge conditions: 13.56 + 27.12 MHz, argon, 2.5 cm electrode gap, $\phi_{lf} = \phi_{hf}$ are kept constant at 300 V, 150 V and 75 V at 6.6 Pa, 20 Pa and 100 Pa, respectively.

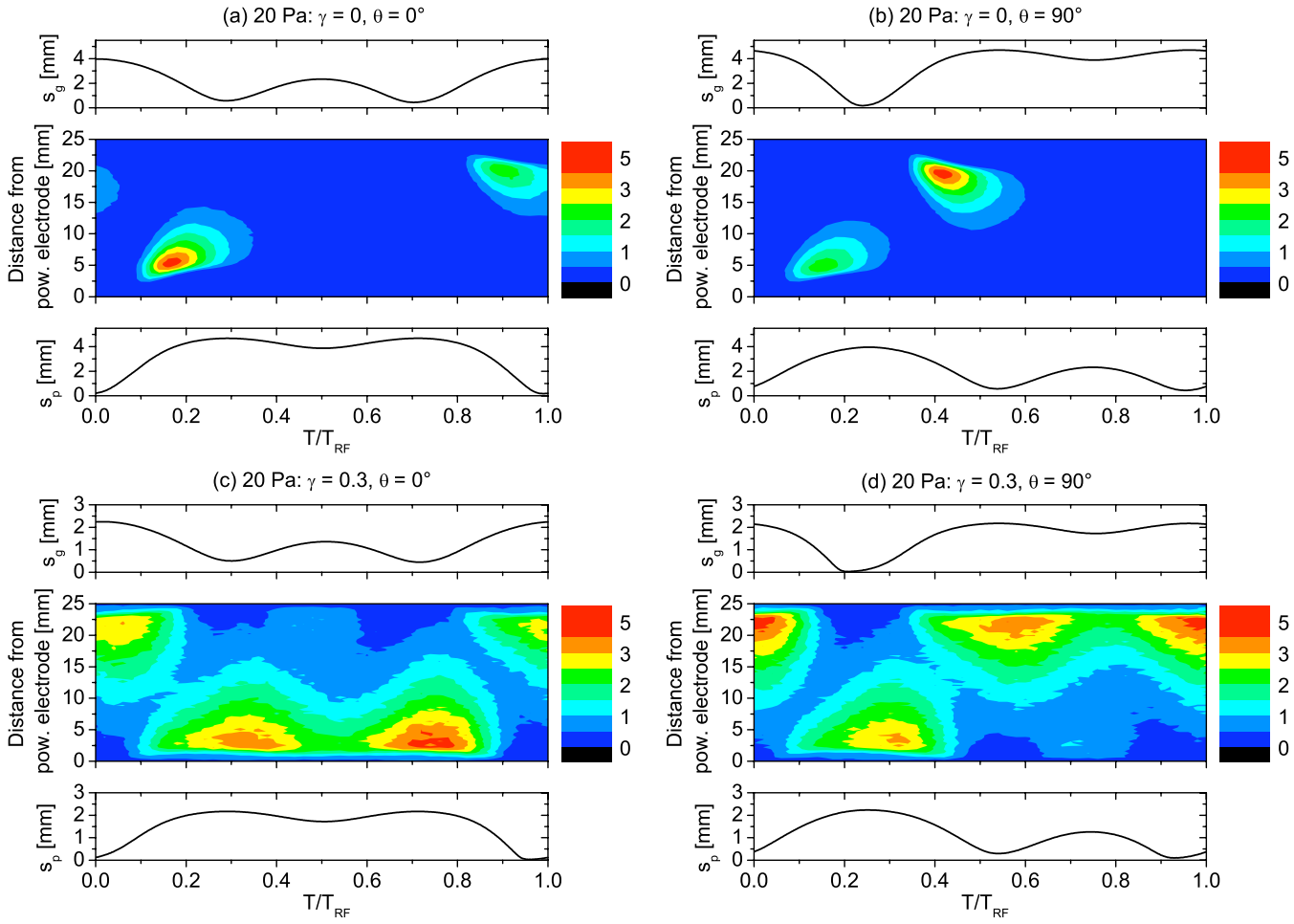

Figure 5. Spatio-temporal distribution of the ionization rate and sheath widths (s_p, s_g) at the powered and grounded electrode as a function of time within one lf period in an electrically asymmetric DF discharge operated in argon at 20 Pa for different values of γ and θ (2.5 cm electrode gap, $\phi_{lf} = \phi_{hf} = 150$ V): (*a*) $\gamma = 0$, $\theta = 0°$, (*b*) $\gamma = 0$, $\theta = 90°$, (*c*) $\gamma = 0.3$, $\theta = 0°$, (*d*) $\gamma = 0.3$, $\theta = 90°$. The color scale is given in 10^{20} m^{-3} s^{-1}.

causes a local enhancement of the ionization rate at one sheath edge for $\theta = 0°$ and 90°. This causes the ion density profile to peak at one sheath edge for $\theta = 0°$ and 90° (asymmetric ionization), while it is flat for $\theta = 60°$ (symmetric ionization). This is depicted in figure 4, which shows the time-averaged ion density profile for different phase shifts, θ, and for the highest values of γ investigated at 6.6 Pa ($\gamma = 0.3$), 20 Pa ($\gamma = 0.3$) and 100 Pa ($\gamma = 0.4$). For the same reason, the ion flux and mean ion density in the sheath are higher at one electrode compared with the other at phase shifts of asymmetric ionization (figure 3). This leads to a decrease in the maximum dc self-bias as a function of γ at high pressures such as shown in figure 3 [26]. A change in the symmetry of the spatio-temporal ionization does not affect the ion flux in this way at

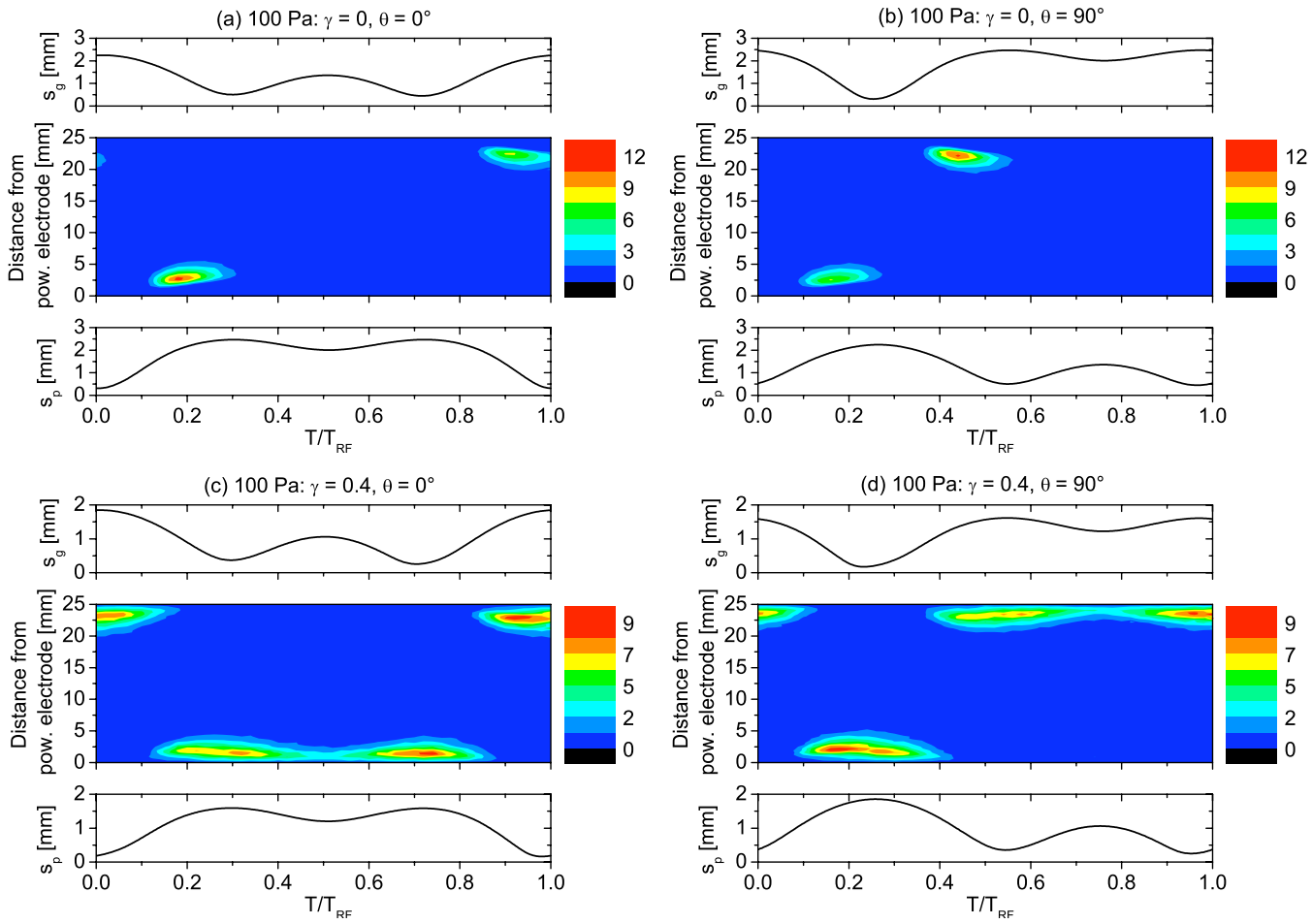

Figure 6. Spatio-temporal distribution of the ionization rate and sheath widths (s_p, s_g) at the powered and grounded electrode as a function of time within one lf period in an electrically asymmetric DF discharge operated in argon at 100 Pa for different values of γ and θ (2.5 cm electrode gap, $\phi_{lf} = \phi_{hf} = 75$ V): (*a*) $\gamma = 0$, $\theta = 0°$, (*b*) $\gamma = 0$, $\theta = 90°$, (*c*) $\gamma = 0.4$, $\theta = 0°$, (*d*) $\gamma = 0.4$, $\theta = 90°$. The color scale is given in 10^{20} m^{-3} s^{-1}.

lower pressures, since the ionization sources are less localized at the sheath edges. Consequently, the ion density profiles are center-peaked instead of edge-peaked at lower pressures (figure 4).

Finally, we discuss the effect of tuning θ on the ion flux at the lowest pressure investigated (6.6 Pa: $\lambda_e \approx l > s_{max}$): under these conditions the EAE allows one to change the mean ion energies by a factor of about 2.4 in EA DF discharges by tuning θ from 0° to 90°, while the ion fluxes at each electrode are basically equal for these two phase shifts of maximum and minimum mean ion energy. For the highest secondary yield investigated ($\gamma = 0.3$) the ion flux is found to peak at $\theta \approx 45°$ in EA DF discharges. At this phase shift, the ion flux is increased by a factor of about 2 compared with $\theta = 0°$ and 90°. Thus, if θ is tuned from 0° or 90° to 45°, the quality of the separate control is strongly reduced for such high values of γ at low pressures.

Nevertheless, the physical origin of this effect might be interesting for other applications. It is understood by an analysis of the spatio-temporal distribution of the ionization rate at $\theta = 0°$, 50° and 90° for $\gamma = 0.3$ shown in figure 7. Note, that the scales for the ionization rates are the same in figures 7(*a*)–(*c*). Secondary electrons, that are generated by ion impact at one electrode, gain energies up to several hundred eVs ($\phi_{lf} = \phi_{hf} = 300$ V). As the ionization mean free path for highly energetic electrons is comparable to the bulk length, most of these electrons arrive at the other electrode after no, or maximum one, ionizing collision in the plasma bulk having transferred only a small fraction of their energy into ionization. These highly energetic electrons are either lost or reflected at the opposing electrode. If they are lost, their remaining energy will also be lost. In the case of reflection, however, they remain inside the discharge and their energy can still be used to ionize, which finally results in a higher plasma density. If these γ-electrons arrive at the opposing electrode, when the sheath at this electrode is collapsed or when the sheath voltage is lower than their kinetic energy, they will hit the electrode and will be reflected with a probability of only 20%. If they arrive at the opposing sheath, when the sheath is expanded and the sheath voltage is higher than their kinetic energy, they will be reflected with a probability of 100%. At $\theta = 0°$ and 90° (figures 7(*a*) and (*c*)), secondary electrons generated at one electrode will mostly arrive at the other electrode at the phase of sheath collapse, i.e. most of them will be lost and, thus, the plasma density and the ion fluxes to the electrodes will be low. In contrast to this scenario, at $\theta = 50°$ secondary

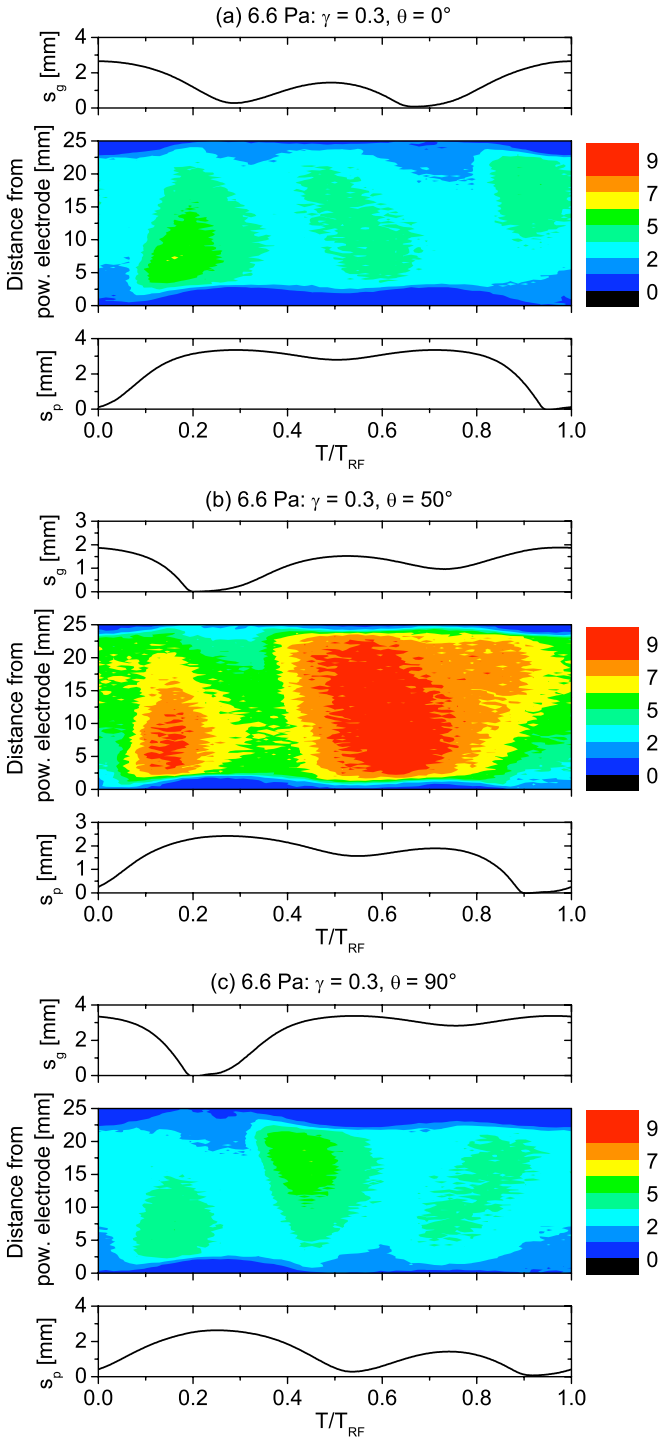

Figure 7. Spatio-temporal distribution of the ionization rate and sheath widths (s_p, s_g) at the powered and grounded electrode as a function of time within one lf period in an electrically asymmetric DF discharge operated in argon at 6.6 Pa for $\gamma = 0.3$ and different values of θ (2.5 cm electrode gap, $\phi_{lf} = \phi_{hf} = 300$ V): (*a*) $\theta = 0°$, (*b*) $\theta = 50°$, (*c*) $\theta = 90°$. The color scale is given in 10^{20} m^{-3}s^{-1}.

electrons will arrive at the opposing electrode at phases of high sheath voltage and will be reflected back into the bulk during a substantial fraction of the lf period. In this way their energy is transferred efficiently into ionization and the plasma density as well as the ion fluxes at both electrodes are significantly increased (figures 3 and 4). This confinement of secondary electrons is similar to the confinement of energetic beam electrons generated by the expanding sheaths in α-mode at low pressures, the so-called electron ping-pong [52, 53, 65]. Here, this effective confinement is caused by the particular choice of the driving voltage waveform at $\theta = 50°$. In essentially all classical CCRF discharges (single-, dual- or multi-frequency discharges) this confinement effect cannot occur due to the choice of either purely sinusoidal voltage waveforms or superpositions of sinusoidal waveforms with significantly different frequencies. This effect is negative for the quality of the separate control of mean ion energy and flux, but it might be useful to generate high-density plasmas at low pressures, e.g. for plasma etching.

The above explanation is further supported by two different arguments: (i) in figure 7(*b*) the ionization is strongly depleted at times of sheath collapse at one of the electrodes, since at these times the highly energetic secondary electrons are no longer confined, but lost to the electrode. (ii) For high values of γ, the mean energy of electrons lost at one electrode is significantly higher at the electrode, where secondary electrons are lost efficiently at phase shifts, θ, of inefficient confinement (figure 8). At $\gamma = 0$, the mean electron arrival energies are essentially identical at both electrodes and independent of θ. With increasing γ the number of secondary electrons generated at each electrode increases and the arrival energies start depending on θ and become different at $\theta = 0°$ and 90° at both electrodes due to a modulation of the confinement quality as a function of θ (figure 8). The mean electron arrival energies do not reach the average energy of the secondary electrons, because even for $\gamma = 0.3$ the total number of secondary electrons is small compared with the number of thermal electrons and only a small fraction of the electrons lost to each electrode are secondary electrons. Based on the work of Wang and Kushner [66, 67] these results might provide a way to control the fluxes of highly energetic electrons into deep etch trenches to neutralize positive charge on the side walls to avoid twisting of etch profiles.

3.3. *Comparison of both discharge types*

Finally, we compare both discharge types with respect to the quality of the separate control of ion properties by defining a control factor for the mean ion energy, f_E, and for the ion flux, f_Γ:

$$f_E = \frac{\langle E_i \rangle}{\langle E_{i,0} \rangle} \tag{4}$$

$$f_\Gamma = \frac{\Gamma_i}{\Gamma_{i,0}}. \tag{5}$$

Here, $\langle E_{i,0} \rangle$ is the mean ion energy at $\phi_{lf} = 0$ V (classical DF discharge) or $\theta = 0°$ (EA DF discharge). $\Gamma_{i,0}$ is a reference ion flux defined as $\Gamma_{i,0} = \Gamma_i(\phi_{lf} = 0\,\text{V})$ in classical DF discharges and $\Gamma_{i,0} = \sum_{k=1}^{N} \Gamma_i^{(k)}/N$ in EA DF discharges, where N is the number of different phase shifts, θ, investigated for a given parameter set. In EA DF discharges, $\Gamma_{i,0}$ corresponds to the mean ion flux. In classical DF discharges, there is no clear definition of a mean ion flux, since there is no upper limit for ϕ_{lf}, while θ is changed between the limits of 0° and 90° in

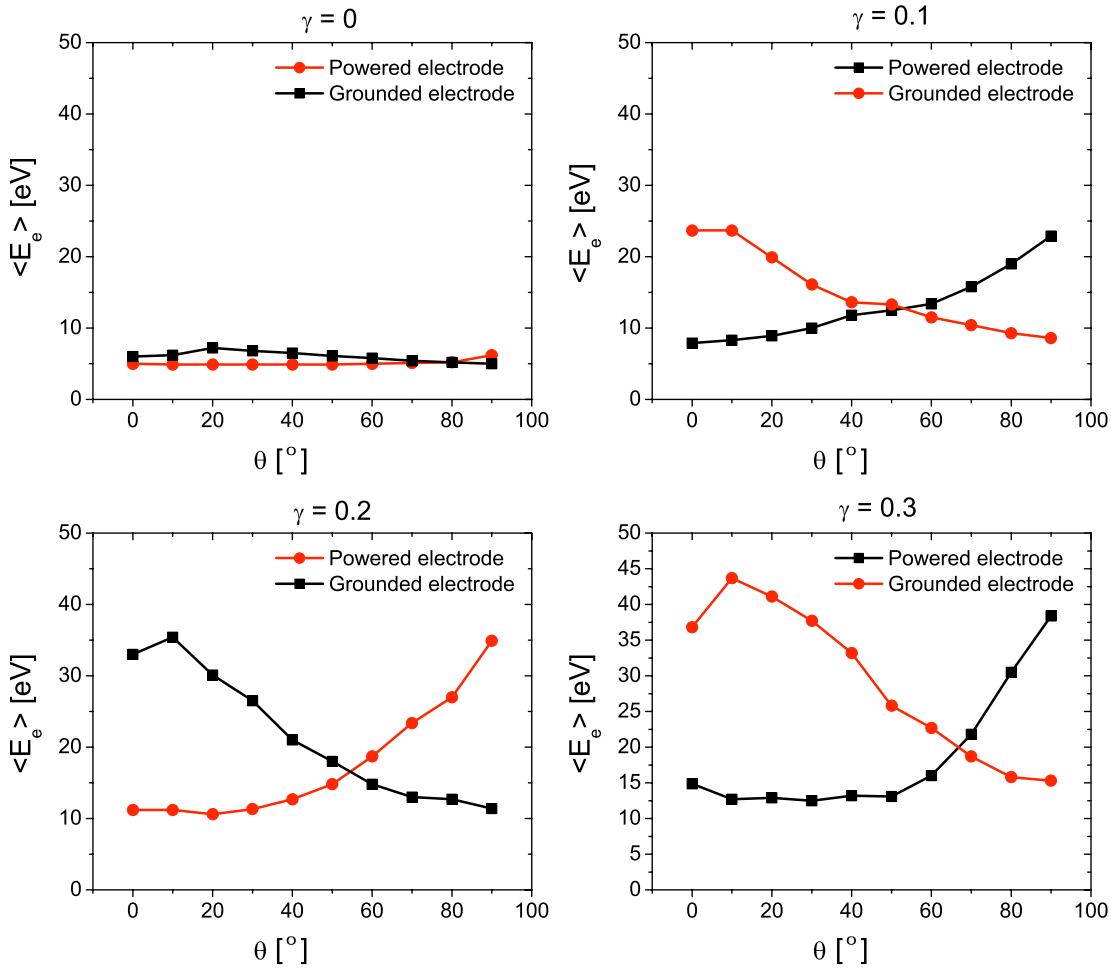

Figure 8. Average energy of electrons lost to each electrode as a function of θ for different values of γ in electrically asymmetric DF discharges operated in argon at 6.6 Pa (2.5 cm electrode gap, $\phi_{\mathrm{lf}} = \phi_{\mathrm{hf}} = 300$ V).

EA discharges. Thus, for the definition of $\Gamma_{i,0}$ in classical DF discharges, the ion flux at $\phi_{\mathrm{lf}} = 0$ V is chosen as the reference flux.

Figure 9 shows f_Γ as a function of f_E for both discharge types at all pressures investigated and for different values of γ. In these plots, $f_\Gamma = 1 \,\forall\, f_E$ corresponds to an ideal separate control. Obviously, under most discharge conditions the quality of the separate control of ion properties is better in EA compared with classical DF discharges. Figure 9 also shows, that f_E, i.e. the control range for the mean ion energy, can be higher in classical compared with EA discharges, since there is principally no upper limit of ϕ_{lf}. This is an advantage of classical DF discharges, although a large change in the mean ion energy is accompanied by a large change in the ion flux for high values of γ. It is noted that the range of ion energy control in EA discharges can be significantly enlarged by adding further consecutive harmonics with customized harmonics' amplitudes to the driving voltage waveform [35, 36]. A detailed investigation of the effect of secondary electrons in such multi-frequency discharges is beyond the scope of this work and remains a topic for future investigations, although many conclusions drawn for DF discharges are expected to be valid in multi-frequency discharges as well. Accordingly, we restrict the presentation of data to a limited range of f_E in figure 9 to focus on the energy range accessible in EA discharges.

In this work, we have focused on the mean ion energy only and not on the ion flux-energy distribution functions. However, for applications the latter quantity might be relevant. While a thorough investigation of this issue is beyond the scope of this work, we note that for the discharge conditions investigated here and for a given mean ion energy, we find the sheaths to be wider in classical compared with EA DF discharges. This is caused by a lower ion density in classical discharges due to the less efficient electron heating caused by the low value of the lower driving frequency. At a given pressure, this causes the sheath and the ion-flux energy distribution functions in classical discharges to be more collisional compared with EA DF discharges.

All discharges investigated in this work are electropositive and operated in pure argon. For applications, complex gas mixtures containing electronegative constituents such as CF_4 or SF_6 are often used. The presence of negative ions can have a marked influence on the ion flux and energies. In strongly electronegative discharges, a high voltage drops across the bulk leading to a high electric field at the discharge center. This high field is required to drive a given current through the bulk, since the conductivity is low due to the low electron density [68–72].

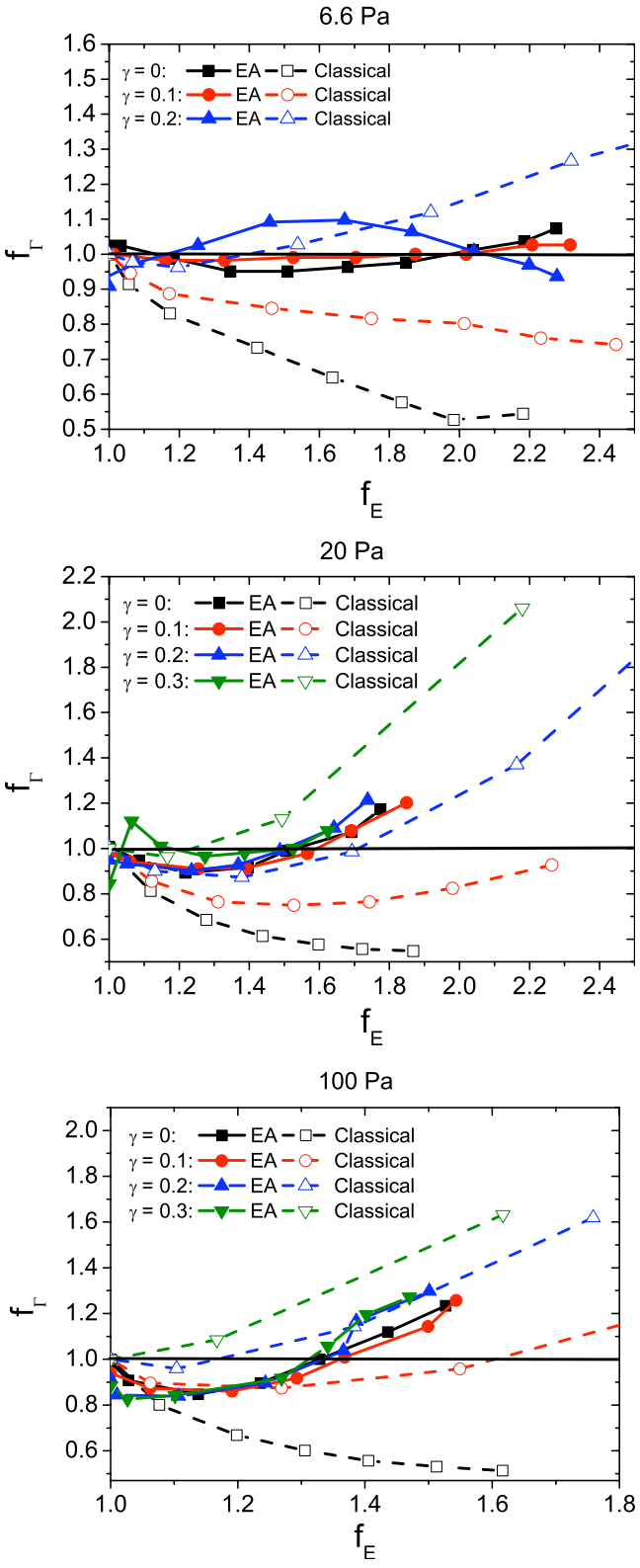

Figure 9. Control factor for the ion flux as a function of the control factor for the mean ion energy in classical as well as electrically asymmetric (EA) discharges at 6.6 Pa (top), 20 Pa (middle) and 100 Pa (bottom) for different values of γ.

This mechanism can cause the discharge to be operated in a bulk heating mode instead of α- or γ-mode, which significantly affects the ionization dynamics and, thus, the ion flux. In EA DF discharges in CF_4, the bulk heating was found to affect the electrical generation of the dc self-bias as a function of θ and, thus, the mean ion energy [72].

4. Conclusions

The effect of secondary electrons on the ionization dynamics and the quality of the separate control of the mean ion energy, $\langle E_i \rangle$, and flux, Γ_i, at the electrodes in classical as well as electrically asymmetric dual-frequency capacitive RF discharges operated in argon has been investigated by PIC/MCC simulations. We have focused on the effect of the control parameter for the mean ion energy, i.e. the low-frequency voltage amplitude, ϕ_{lf}, in classical discharges and the phase shift, θ, between the driving harmonics in electrically asymmetric discharges, on the ion fluxes at both electrodes.

We have found that secondary electrons induce a mode transition of the electron heating and ionization dynamics from α- to γ-mode as a function of the control parameter for the mean ion energy, ϕ_{lf}, in classical dual-frequency discharges. This is caused by an increase in the sheath voltages and widths (for a given ion density profile) and, thus, a more effective generation and multiplication of highly energetic secondary electrons as a function of ϕ_{lf}. Consequently, the ion fluxes at both electrodes increase dramatically as a function of the control parameter for the mean ion energy in the presence of secondary electrons, i.e. for high values of γ. This increase is strongest if $\phi_{lf} > \phi_{hf}$, i.e. under typical operating conditions of classical dual-frequency discharges. Thus, separate control of the mean ion energy and flux at the electrodes is impossible in classical dual-frequency discharges for high values of γ, since the principal idea of decoupling ion acceleration and electron heating by choosing $\phi_{lf} > \phi_{hf}$ fails. Due to the additional limitations caused by the frequency coupling in the absence of secondary electrons we conclude that (except within some rather narrow process windows, where the effects of secondary electrons and the frequency coupling compensate) under most discharge conditions classical DF discharges do not allow a separate control of mean ion energy and flux at the electrodes.

Instead, we have found electrically asymmetric DF discharges to allow a qualitatively much better separate control of $\langle E_i \rangle$ and Γ_i due to the fundamentally different concept to control the mean ion energies at both electrodes by tuning θ at fixed voltage amplitudes. In this way, any frequency coupling and mode transition induced by the control parameter for $\langle E_i \rangle$ is avoided. Instead, only the symmetry of the spatio-temporal ionization, but not its mode, is changed by tuning θ.

Deviations from an ideal separate control in these discharges are found at the highest and lowest pressures investigated. At low pressures the quality of secondary electron confinement is changed by tuning θ due to a change in the driving voltage waveform, which affects the sheath motion. Poor confinement is found at $\theta = 0°$ and 90°, while good confinement is observed at $\theta \approx 45°$, since high sheath voltages at both electrodes prevent secondary electrons to be lost to the electrodes during a long fraction of one period of the fundamental frequency. This effect causes the ion fluxes at both electrodes to increase by a factor of about 2 at $\theta \approx 45°$ compared with $\theta = 0°$ and 90°. Under these conditions, the

quality of the separate control is reduced, but high-density plasmas can be generated capacitively at low pressures using this effect, e.g. for applications of plasma etching.

Despite these limitations the quality of the separate control of the mean ion energy and flux at the electrodes is generally better in electrically asymmetric discharges compared with classical DF discharges under most discharge conditions investigated.

Acknowledgments

This work has been funded by the Alexander von Humboldt Foundation, the Ruhr-University Research Department Plasma and the Hungarian Scientific Research Fund through grants OTKA-K-77653 and IN-85261. Parts of the project have been supported by the German Federal Ministry for the Environment, Nature Conservation, and Nuclear Safety (O32521OB).

References

[1] Lieberman M A and Lichtenberg A J 2005 *Principles of Plasma Discharges and Materials Processing* 2nd edn (Hoboken, NJ: Wiley Interscience)
[2] Makabe T and Petrović Z Lj 2006 *Plasma Electronics: Applications in Microelectronic Device Fabrication* (London: Taylor and Francis)
[3] Kalache B , Kosarev A I, Vanderhaghen R and Roca i Cabarrocas P 2002 *J. Non-Cryst. Solids* **299** 63
[4] Kroll U, Shah A, Keppner H, Meier J, Torres P and Fischer D 1997 *Sol. Energy Mater. Sol. Cells* **48** 343
[5] Roschek T, Repmann T, Muller J, Rech B and Wagner H 2002 *J. Vac. Sci. Technol.* A **20** 492
[6] Jiang W, Xu X, Dai Z-L and Wang Y-N 2008 *Phys. Plasmas* **15** 033502
[7] Kawamura E, Lichtenberg A J and Lieberman M A 2008 *Plasma Sources Sci. Technol.* **17** 045002
[8] Kawamura E, Lieberman M A, Lichtenberg A J and Hudson E A 2007 *J. Vac. Sci. Technol.* A **25** 1456
[9] Wang S-B and Wendt A E 2000 *J. Appl. Phys.* **88** 643
[10] Patterson M M, Chu H Y and Wendt A E 2007 *Plasma Sources Sci. Technol.* **16** 257
[11] Rauf S and Kushner M J 1999 *IEEE Trans. Plasma Sci.* **27** 1329
[12] Dudin S V, Zykov A V, Polozhii K I and Farenik V I 1998 *Tech. Phys. Lett.* **24** 881
[13] Georgieva V and Bogaerts A 2006 *Plasma Sources Sci. Technol.* **15** 368
[14] Lee S H, Tiwari P K and Lee J K 2009 *Plasma Sources Sci. Technol.* **18** 025024
[15] Lisovskiy V, Booth J P, Landry K, Douai D, Cassagne V and Yegorenkov V 2008 *Plasma Sources Sci. Technol.* **17** 025002
[16] Mussenbrock T, Ziegler D and Brinkmann R P 2006 *Phys. Plasmas* **13** 083501
[17] Kawamura E, Lieberman M A and Lichtenberg A J 2006 *Phys. Plasmas* **13** 053506
[18] Boyle P C, Ellingboe A R and Turner M M 2004 *Plasma Sources Sci. Technol.* **13** 493
[19] Kitajima T, Takeo Y, Petrović Z Lj and Makabe T 2000 *Appl. Phys. Lett.* **77** 489
[20] Denda T, Miyoshi Y, Komukai Y, Goto T, Petrović Z Lj and Makabe T 2004 *J. Appl. Phys.* **95** 870
[21] Yang Y and Kushner M J 2010 *Plasma Sources Sci. Technol.* **19** 055011
[22] Yang Y and Kushner M J 2010 *Plasma Sources Sci. Technol.* **19** 055012
[23] Olevanov M, Proshina O, Rakhimova T and Voloshin D 2008 *Phys. Rev.* E **78** 026404
[24] Voloshin D, Proshina O and Rakhimova T 2010 *J. Phys.: Conf. Ser.* **207** 012026
[25] Heil B G, Schulze J, Mussenbrock T, Brinkmann R P and Czarnetzki U 2008 *IEEE Trans. Plasma Sci.* **36** 1404
[26] Heil B G, Czarnetzki U, Brinkmann R P and Mussenbrock T 2008 *J. Phys. D: Appl. Phys.* **41** 165202
[27] Donkó Z, Schulze J, Heil B G and Czarnetzki U 2008 *J. Phys. D: Appl. Phys.* **42** 025205
[28] Czarnetzki U, Heil B G, Schulze J, Donkó Z, Mussenbrock T and Brinkmann R P 2009 *J. Phys.: Conf. Ser.* **162** 012010
[29] Schulze J, Schüngel E, Donkó Z and Czarnetzki U 2009 *J. Phys. D: Appl. Phys.* **42** 092005
[30] Donkó Z, Schulze J, Czarnetzki U and Luggenhölscher D 2009 *Appl. Phys. Lett.* **94** 131501
[31] Longo S and Diomede P 2009 *Plasma Process. Polym.* **6** 370
[32] Schulze J, Schüngel E, Donkó Z and Czarnetzki U 2009 *J. Appl. Phys.* **106** 063307
[33] Schulze J, Schüngel E, Donkó Z and Czarnetzki U 2010 *Plasma Sources Sci. Technol.* **19** 045028
[34] Schulze J, Schüngel E, Donkó Z and Czarnetzki U 2010 *J. Phys. D: Appl. Phys.* **43** 225201
[35] Schulze J, Schüngel E, Donkó Z and Czarnetzki U 2011 *Plasma Sources Sci. Technol.* **20** 015017
[36] Johnson E V, Verbeke T, Vanel J C and Booth J P 2010 *J. Phys. D: Appl. Phys.* **43** 412001
[37] Czarnetzki U, Schulze J, Schüngel E and Donkó Z 2011 *Plasma Sources Sci. Technol.* **20** 024010
[38] Zhang Q Z, Jiang W, Hou L J and Wang Y N 2011 *J. Appl. Phys.* **109** 013308
[39] Gans T, Schulze J, O'Connell D, Czarnetzki U, Faulkner R, Ellingboe A R and Turner M M 2006 *Appl. Phys. Lett.* **89** 261502
[40] Schulze J, Gans T, O'Connell D, Czarnetzki U, Ellingboe A R and Turner M M 2007 *J. Phys. D: Appl. Phys.* **40** 7008
[41] Schulze J, Donkó Z, Luggenhölscher D and Czarnetzki U 2009 *Plasma Sources Sci. Technol.* **18** 034011
[42] Turner M M and Chabert P 2006 *Phys. Rev. Lett.* **96** 205001
[43] Waskoenig J and Gans T 2010 *Appl. Phys. Lett.* **96** 181501
[44] Donkó Z, Schulze J, Hartmann P, Korolov I, Czarnetzki U and Schüngel E 2010 *Appl. Phys. Lett.* **97** 081501
[45] Donkó Z 2007 *Proc. Symp. of Application of Plasma Processes (Podbanske, Slovakia)* IL02, pp 21–4
[46] Donkó Z and Petrović Z Lj 2006 *Japan. J. Appl. Phys.* **45** 8151
[47] Booth J P, Curley G, Marić D and Chabert P 2010 *Plasma Sources Sci. Technol.* **19** 015005
[48] Belenguer Ph and Boeuf J P 1990 *Phys. Rev.* A **41** 4447
[49] Turner M M, Chabert P, Levif P, Boyle P and Robiche J 2007 *Proc. 18th ICPIG (Prague, Czech Republic)* G08
[50] Böhm C and Perrin J 1993 *Rev. Sci. Instrum.* **64** 31
[51] Phelps A V and Petrović Z Lj 1999 *Plasma Sources Sci. Technol.* **8** R21
[52] Schulze J, Heil B G, Luggenhölscher D, Czarnetzki U and Brinkmann R P 2008 *J. Phys. D: Appl. Phys.* **41** 042003
[53] Schulze J, Heil B G, Luggenhölscher D and Czarnetzki U 2008 *IEEE Trans. Plasma Sci.* **36** 1400
[54] Schulze J, Heil B G, Luggenhölscher D, Brinkmann R P and Czarnetzki U 2008 *J. Phys. D: Appl Phys.* **41** 195212
[55] Rauf S, Bera K and Collins K 2010 *Plasma Sources Sci. Technol.* **19** 015014
[56] Vender D and Boswell R W 1992 *J. Vac. Sci. Technol.* A **10** 1331
[57] Wood B P 1991 *PhD Thesis* University of Berkeley, CA
[58] Boyle P C, Ellingboe A R and Turner M M 2004 *J. Phys. D: Appl. Phys.* **37** 697
[59] Georgieva V and Bogaerts A 2005 *J. Appl. Phys.* **98** 023308

[60] Kollath R 1956 *Encyclopedia of Physics* vol XXI, ed S Flügge (Berlin: Springer) p 264
[61] Phelps A V 1994 *J. Appl. Phys.* **76** 747
[62] Phelps A V http://jilawww.colorado.edu/∼avp/collision_data/ unpublished
[63] Brinkmann R P 2007 *J. Appl. Phys.* **102** 093302
[64] Turner M M 2009 *J. Phys. D: Appl. Phys.* **42** 194008
[65] Schulze J, Schüngel E, Donkó Z and Czarnetzki U 2010 *J. Phys. D: Appl. Phys.* **43** 124016
[66] Wang M and Kushner M J 2010 *J. Appl. Phys.* **107** 023308
[67] Wang M and Kushner M J 2010 *J. Appl. Phys.* **107** 023309
[68] Denpoh K and Nanbu K 1998 *J. Vac. Sci. Technol.* A **16** 1201
[69] Proshina O V, Rakhimova T V, Rakhimov A T and Voloshin D G 2010 *Plasma Sources Sci. Technol.* **19** 065013
[70] Denpoh K and Nanbu K 2000 *Japan. J. Appl. Phys.* **39** 2804
[71] Gogolides E and Sawin H H 1992 *J. Appl. Phys.* **72** 3971
[72] Schulze J, Derzsi A and Donkó Z 2011 *Plasma Sources Sci. Technol.* **20** in press